Composites & nanocomposites



Composite materials made from glass microballoons and ceramic nanofibers for use as catalysts and catalyst supports

M. Armstrong^{1,*} , S. Nealy³, C. Severino¹, W. Maniukiewicz², M. Modelska², M. Binczarski², I. Witonska², K. K. Chawla¹, and A. Stanishevsky³

Received: 13 January 2020 Accepted: 10 June 2020 Published online: 19 June 2020

© Springer Science+Business Media, LLC, part of Springer Nature 2020

ABSTRACT

Glass microballoons (GMBs) are commonly used to reduce the density of epoxyresin syntactic foams, but they can also be applied as a low-cost and lightweight catalyst support. In order to create a practical structure that can be utilized for such an application, a ceramic syntactic foam consisting of glass microballoons (GMBs) and silica nanofibers (NFs) with or without TiO2 binder was synthesized. The mechanical strength, phase composition, high-temperature deformation behavior, and microstructure of the composite material were analyzed using bending and compression tests, X-ray diffraction, and scanning electron microscopy, respectively. It was determined that the addition of nanofibers improves the thermal behavior and mechanical strength of the composite material during and after processing. The composite materials maintained up to 70% anatase titania at as high as 700 °C, and this indicates that they can be of interest for high-temperature catalysis. No high-temperature deformation of GMBs was observed at 800 °C or 1000 °C, whereas XRD of samples coated with TiO₂ using a titanium oxysulfate solution indicated the formation of cristobalite above 800 °C. Preliminary methane-reforming experiments were performed with NiO-seeded titania-coated GMBs, uncoated GMBs, and an uncoated silica fibers/GMBs composite. Uncoated GMBs and titania-coated GMBs had a low conversion ratio of methane to products, but the uncoated composite structure showed high conversion of the reactants at high temperatures, indicating that it may be suitable catalyst support in this reaction.



¹ Department of Materials Science and Engineering, University of Alabama at Birmingham, 1150 10th Ave S, Birmingham, AL 35205, USA

² Faculty of Chemistry, Łódź University of Technology, Stefana Żeromskiego 116, 90-924 Łódź, Poland

³ Department of Physics, University of Alabama at Birmingham, 1300 University Blvd, Birmingham, AL 35233, USA

Introduction

Glass microballoons (GMBs), hollow silica spheres averaging 40 µm in diameter with a wall thickness of 2–3 µm, are a common material employed to reduce the weight of composite syntactic foams [1–3]. The majority of syntactic foams utilize GMBs in an epoxyresin matrix. GMBs are preferable for such an application as their round shape prevents stress concentration and allows for a large decrease in weight with a relatively small decrease in mechanical properties [3, 4]. While these foams are common for use in structural applications, it may be possible to utilize the concept of syntactic foams for other technical applications, such as inorganic catalyst support [5–7] or electromagnetic interference shielding [8]. GMBs have been shown to be a suitable support material for TiO_2 and TiO_2/Ag_3PO_4 photocatalysts [5, 7], so a kind of syntactic foam may be possible using the active catalysts, such as transition metal oxides, as an inorganic binder between the GMBs. Furthermore, GMBs have demonstrated the potential as the support for highly dispersed catalytic particles [6]. By combining an inorganic binder/catalyst and catalysts nanoparticles, a lightweight material with a high surface area could be developed for catalyst support applications. For example, the material may also hold potential for the dispersion of transition metal-based catalysts, such as nickel or NiO. Many processes that use nickel-based catalysts, such as methane reforming and CO₂ methanation, are hindered by sintering of the nickel particles at high temperatures [9]. Silica, specifically mesoporous SBA-15, has been shown to be a suitable support for nickel in these applications as dispersion of the nickel particles prevents sintering and allows for the preservation of a greater number of active sites [10-14]. As such, GMBs may have similar success as a support material for nickel and NiO.

A major concern in the development of any syntactic foam is the mechanical strength, as they often consist of a brittle reinforcement within a brittle polymer matrix [15]. In epoxy-resin syntactic foams, carbon fiber has been shown to increase the mechanical strength of the composite material, particularly in tension [4, 15–19]. These systems often add 1–5% of carbon fiber or carbon nanofibers to the existing foam, and the addition of the fibers strengthens the material through crack bridging, crack blunting, and the transfer of load from the

matrix to the fibers [15, 19–23]. While adding carbon or silica (SiO₂) fibers has consistently been shown to improve the mechanical properties of epoxy-resin syntactic foams [15], the mechanisms that allow for this phenomenon would not be present in a syntactic foam where the matrix is a coating on the reinforcement rather than a bulk material. In this case, it is expected that the delamination of the coating from the reinforcement will play a crucial role in the mechanical strength of the syntactic foam, and the strength will also be largely dependent on the contact area between the individual GMBs. Although the mechanisms for fracture may not be the same between these materials, fibers, specifically short nanofibers, may strengthen the material by increasing the packing density of the reinforcement and providing a greater contact area between GMBs [15]. By providing more area for the inorganic binder to join the base components of the composite, fibers may increase the mechanical strength and handleability of a fully inorganic syntactic foam. The fibers will also drastically increase the available surface area for catalyst deposition, which may increase the number of active sites and the activity of the catalyst.

In this work, the possible synthesis process of a fully ceramic syntactic foam has been explored, and the effect of the addition of SiO₂ nanofibers, a material compositionally similar to GMBs, on the structural integrity of such a structure has been determined. Preliminary tests on the viability of these materials for catalyst support applications in steam reforming of methane with Ni-based nano-catalyst have been performed.

Experimental methods

Materials

Glass microballoons (GMBs, Eccospheres SID-230Z, Trelleborg) with an average diameter 40 μ m were purchased from Fischer Scientific. Tetraethoxysilane (TEOS, Si(OC₂H₅)₄, 99%+ , Alfa Aesar) and polyvinyl butyral (PVB, $M_{\rm w} \sim 70,000$, 80% butyral, Scientific Polymer Products, Inc) were used to fabricate silica nanofibers using a high-yield alternating field electrospinning [24]. Hydrochloric acid (5 N) and ethanol (200 proof) were supplied by Fischer Scientific and Decon Labs, Inc., respectively. DI water was produced on-site. Titanium butoxide (Ti(OBu)₄,



 $Ti[O(CH_2)_3CH_3]_4$, 99%+, Alfa Aesar), polyvinylpyrrolidone (PVP, M_w 1,300,000, Alfa Aesar), hydroxypropyl cellulose (HPC, M_w 100,000, Alfa Aesar), and titanium oxysulfate (TiOSO₄, Sigma Aldrich) were used to prepare the TiO₂ binder.

Fabrication of composites

The concept for the composite synthesis is demonstrated in Fig. 1, which shows the support materials, GMBs and silica nanofibers, being combined and coated with a titania layer (shown in red) to act as both a binder and an active ingredient. Composite samples were synthesized by combining dry mixtures of glass microballoons and chopped silica nanofibers with a titania-based binder solution. Two variations of the binder solutions were tested: a titanium(IV) butoxide-based solution and a titanium(IV) oxysulfate-based solution. The titanium(IV) butoxide-based solution (CS1) consisted of a mixture of titanium(IV) butoxide, ethanol, acetic acid, and polyvinylpyrrolidone (PVP) in 0.05/6.5/0.05/0.036 molar ratio. The titanium(IV) oxysulfate-based solution (CS2) consisted of a mixture of titanium(IV) oxysulfate, PVP, and DI water with ratios found in Table 1.

For mechanical testing, the composite samples were prepared in the shape of rectangular slabs (approximately $25 \times 6 \times 3$ mm) and cylindrical slabs (13 mm diameter and 3 mm thick) by pouring the

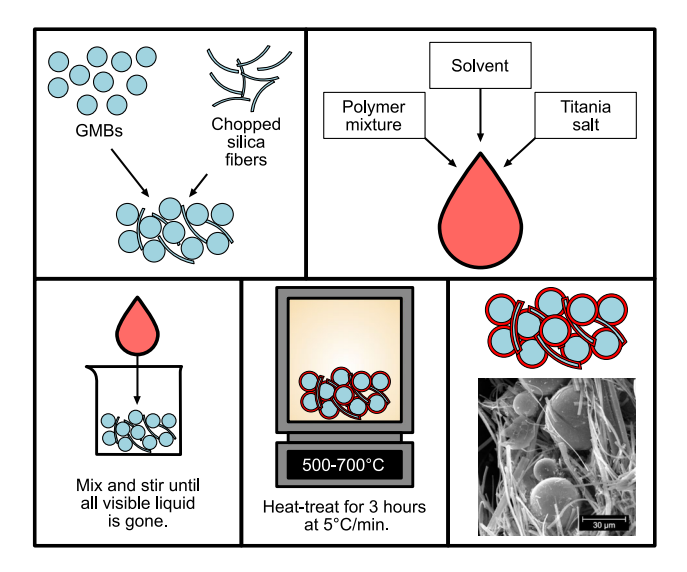


Figure 1 An illustration of the process used to synthesize the syntactic foam. It shows the base materials (GMBs and SiO_2 nanofibers) being combined and then coated in TiO_2 .

Table 1 Coating solutions per 300 mg of fiber-based syntactic foams with varying fiber/GMB ratios

Fiber/GMB ratio	TiOSO ₄ (mg)	PVP (mg)	Water (mL)
0:1	24	15	1
1:1	72	23	1
1:0	120	30	1

Amounts of polymer (PVP) and salt (TiOSO₄) were adjusted to account for variations in surface area of the substrate components

GMB/silica nanofiber suspensions into aluminum alloy molds. They were then left to dry for at least 24 h in a desiccator at room temperature. The resulting slabs were removed from the mold, heated at 1.5 to 2.5 °C/min to 500 °C, and kept at 500 °C for 3 h.

Characterization

A Tescan Vega3 scanning electron microscope (SEM) was used for analysis of the NF/GMB interactions and effectiveness of the titania coating. The samples were sputter-coated to reduce surface charging effect in SEM and imaged in a secondary electron mode at 30 kV voltage. For analysis of the catalyst-seeded samples, images were taken using a Hitachi S-4700 SEM equipped with a Thermo Noran energy-dispersive diffractometer. In this case, images were taken in backscattered electron mode at 25 kV voltage.

A PANalytical X'Pert Pro MPD diffractometer (Cu Kα tube operated at 40 kV and 45 mA, PANalytical X'Celerator detector, the Bragg–Brentano geometry) was used to obtain X-ray diffraction (XRD) patterns of the composites. Data were acquired over the range of 5°-90° 2θ using the step of 0.0167° and dwell time of 27 s. Powdered samples were pressed into the holders and rotated during the measurements to minimize the possibility of preferred orientation effects. Crystalline phases and crystallite size were determined using the PANalytical High Score Plus software package and the International Centre for Diffraction Data (ICDD) powder diffraction file (PDF-2 ver. 2009) database. This method was utilized to determine the phase composition of the titania in the samples as well as the effectiveness of catalyst seeding on the GMBs.



Catalyst reactions

For the preliminary catalytic tests on methane reforming, the fiber/GMB suspensions were stirred in an open beaker until fully dried, then heated at 5 °C/min, and calcined at 500 °C or 700 °C for 2 h. The three types of samples were uncoated GMBs, titania-coated GMBs, and a 1:1 mixture of silica fibers and GMBs. Coated GMBs were synthesized by combining 30 g of GMBs with 20 mL of CS1 solution, stirring until dry, and then calcining at 500 °C for 2 h at 5 °C/min. The samples were seeded with nickel oxide by adding a solution of 0.4955 g of Ni(NO₃)₂₋ 6H₂O in water to 2 g of the support material and drying the sample in a round-bottom flask at 60 °C. The intended nickel concentration was 5 mol%. The samples were then heated to 110 °C in an air for six hours to remove any remaining moisture; then, they were heated to 500 °C in oxygen for calcination to form NiO. The heating rate between all processing steps was 20 °C per minute. The catalysts were placed in NiO form in a catalytic reactor and there partially reduced in the atmosphere of the gases used in the reaction.

In order to determine the amount of Ni that was deposited on the surface of the base materials, the chemical composition of the samples was analyzed using a Unicam Instruments SOLAAR M6 spectrometer to perform atomic absorption spectroscopy (AAS). Samples were prepared for this analysis by adding 0.1 g of the material to a mixture of nitric (V), hydrochloric, and hydrofluoric acids in an MLS-1200 Mega Microwave Digestion System. The nickel content in the samples was determined using an analytical wavelength of 352.4 nm after atomization in an acetylene/air flame.

The oxy-steam reforming of methane was performed in a quartz micro-reactor at two temperatures 700 °C and 900 °C and under atmospheric pressure. Catalytic activity was measured after reaching a stable state of the catalyst system after 30 min of the process. The weight of a catalyst test sample was 0.1 g. A volumetric ratio between each component of the reaction mixture was the following: CH₄:H₂-O:O₂ = 1:2.7:0.35. Argon was used as a balance gas. The total gas flow rate of the reaction mixture was 51 ± 0.2 mL/min. The analysis of the gaseous reaction mixture composition before and after the reaction was monitored using gas chromatographs

equipped with a thermal conductivity detector (TCD) and a flame ionization detector (FID).

Mechanical testing

Flexural strength of the samples was conducted using a three-point bending test. Depending on length of the finished sample, a gauge length of either 8 mm or 18 mm was used. Tests were conducted with three samples of each type using a custom-made tester based on an Omega DFG35-1 N force gauge at the strain applied in 10 μ m increments until failure was achieved. Compression tests of the samples were conducted using a Mark-10 M3-5 25 N force gauge in increments of 10 μ m. Load was applied using ceramic cylinders 1.55 \pm 0.05 mm and 3 \pm 0.05 mm in diameter.

Results

Scanning electron microscopy

Coating analysis

SEM images of eight samples coated with CS1 are shown in Fig. 2. These images show how both the relationship between the silica fibers and the glass microballoons, and the behavior of the titania coating changed based on fiber content and temperature. None of the images show any significant interaction between the fibers and the GMBs, rather the GMBs are merely contained in somewhat of a nest-like fibrous structure in compositions with a high fiber content, such as in Fig. 2d. It can also be noted that some silica fibers trend to wrap around the GMBs. The TiO₂ coating appears to delaminate from the GMBs at both 500 °C and 700 °C, indicating that this particular coating solution may not be suitable to coat these substrates. SEM images of three samples coated with CS2 are shown in Fig. 3. In all of the images, it is clear that there has been no delamination of the coating, and in Fig. 3b, the same nest-like fibrous structure as those in Fig. 2 can be seen. EDS analysis of these samples (discussed later in the text) confirms the existence of a titania coating. Between CS1 and CS2, these images indicate that CS2 aqueous binder solution was more successful at achieving a uniform coating of titania [25].



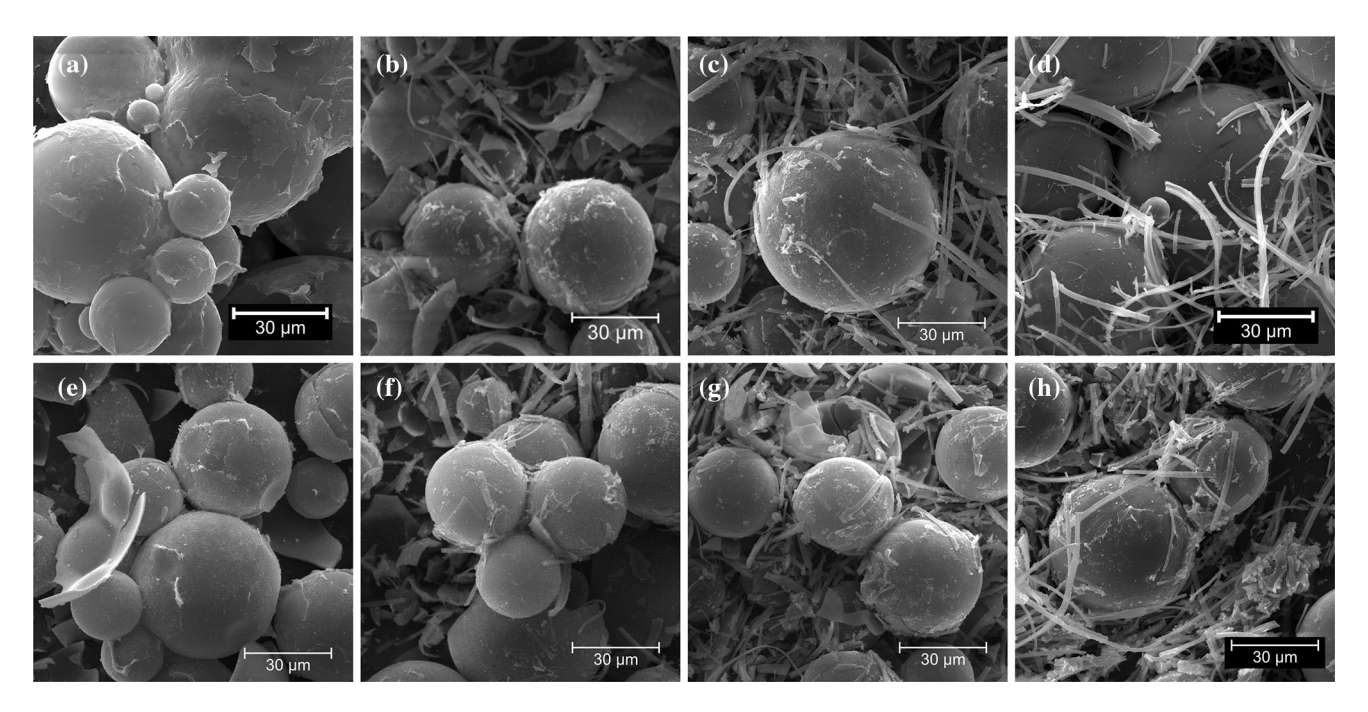


Figure 2 SEM images of silica fiber/GMB composites with the following mass ratios of fibers to GMBs and processing temperatures: **a** 0:1 at 500 °C, **b** 1:3 at 500 °C, **c** 1:1 at 500 °C, **d** 3:1 500 °C, **e** 0:1 at 700 °C, **f** 1:3 at 700 °C, **g** 1:1 at 700 °C, **h** 3:1 at 700 °C.

High-temperature deformation of GMBs

SEM images of samples treated at 800 °C and 1000 °C are shown in Fig. 3. It has been established that silica nanofibers are stable up to 1000 °C [24]. Samples were analyzed with and without a coating to determine whether there was any effect of the coating on high-temperature deformation of GMBs. Of the eight samples in the figure, none of them appear to have deformed despite exposure to high temperatures for an extended period of time, which was not expected, as GMBs tend to soften around 600 °C.

NiO seeding of GMBs and GMB/fiber composites

Figure 4 shows SEM images and EDS maps of the three NiO-seeded samples. These maps show that, while all of the samples had NiO particles evenly dispersed on the surface of the base materials, the sample comprised of uncoated GMBs had a noticeably sparser population of NiO particles compared to the other two samples.

X-ray diffraction

CS1 samples

XRD patterns for four samples annealed at 500 °C are shown in Fig. 5a, and patterns for two samples annealed at 700 °C are shown in Fig. 5b. In Fig. 5a, the samples all have a pronounced peak at $2\theta = 25.2^{\circ}$, which indicates the formation of the TiO₂ anatase phase. In Fig. 5b, the samples show a small peak at $2\theta = 27.4^{\circ}$ in addition to the larger peak at $2\theta = 25.2^{\circ}$, which indicates the presence of the TiO₂ rutile phase (approximately 25–30%). A broad maximum centered around $2\theta = 22^{\circ}$ indicates amorphous silica, which corresponds to the composition of both the GMBs and silica fibers. In Fig. 5a, it appears that the titania peaks become smaller as fiber content increases, but this discrepancy is eliminated when the peaks are normalized in relation to the silica peak.

CS2 samples

Due to apparently better coating capability of CS2 binder solution, dynamic XRD patterns were recorded during the calcination at different temperatures to better understand the development of the TiO₂ layer microstructure. Figure 5 displays dynamic XRD patterns for samples coated with TiO₂ using CS2



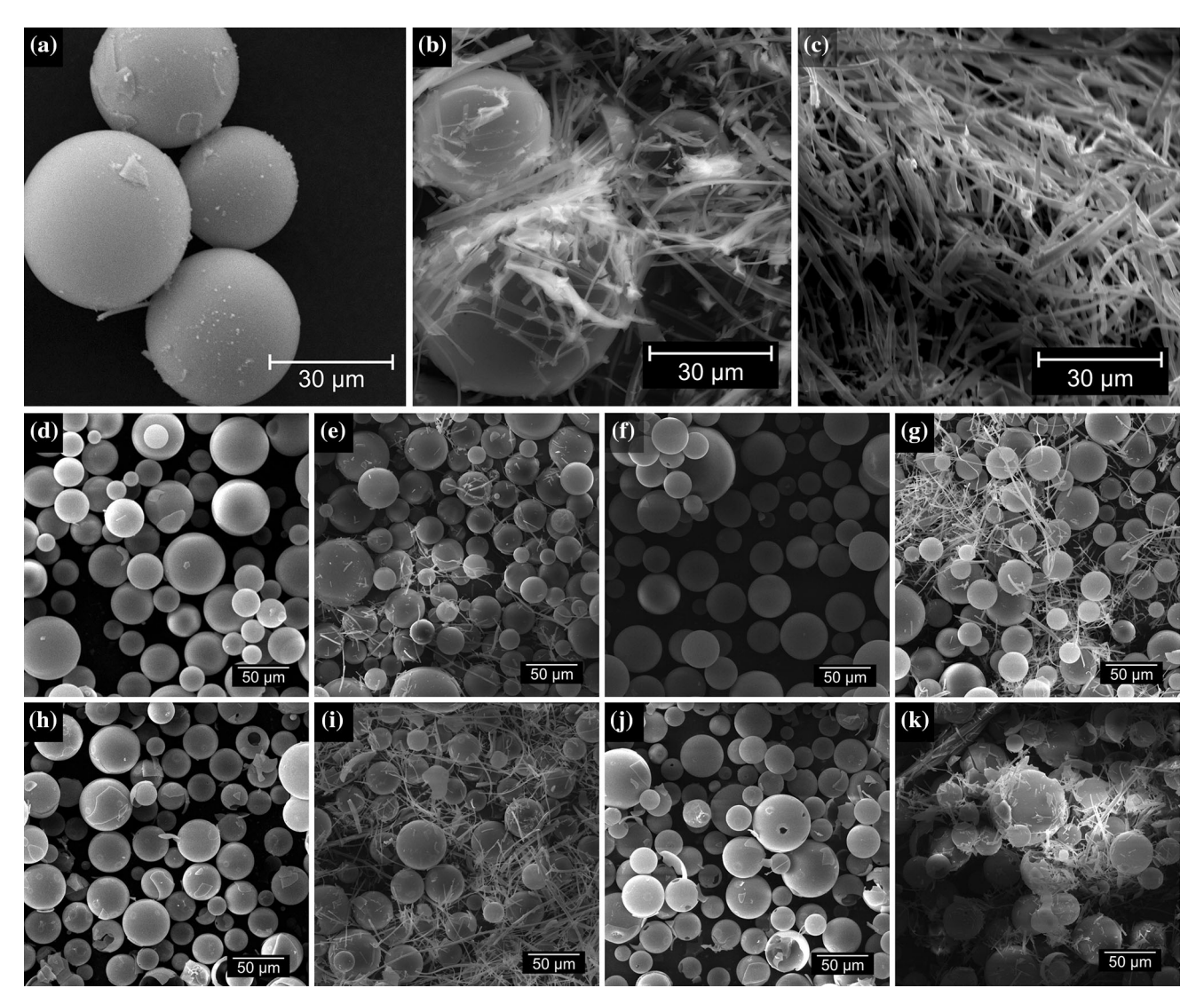


Figure 3 SEM images of syntactic foams synthesized using CS2. **a–c** demonstrate a uniform coating on both the GMBs and the nanofibers and binding between the two components and depict syntactic foams with the following ratios of components: **a** 100% GMBs, **b** 1:1 nanofibers/GMBs, and **c** 100% nanofibers. **d–k** show syntactic foams subjected to high temperatures taken to

solution, with each pattern representing the same fiber/GMB sample at various temperatures. Figure 5c presents XRD patterns of a 0:1 fiber/GMB sample from 500 °C to 850 °C, which contain the characteristic peak for anatase titania at every temperature, the characteristic peak for rutile titania appears above 650 °C, and a sharp peak appears at $2\theta = 21.9^{\circ}$ at 800 °C that indicates the formation of cristobalite. Figure 5d shows the XRD patterns of a 1:1 fiber/GMB sample, which contain the characteristic peak for anatase titania at every temperature and

analyze the deformation behavior of the components. Samples **d**–**g** have been coated with titania, and samples **h**–**k** are uncoated. The samples in each picture contain the following nanofiber/GMB ratios and are processed at the following temperatures: **d** 0:1 at 800 °C, **e** 1:1 at 800 °C, **f** 0:1 at 1000 °C, **g** 1:1 at 1000 °C, **h** 0:1 at 800 °C, **i** 1:1 at 800 °C, **j** 0:1 at 1000 °C, and **k** 1:1 at 1000 °C.

the characteristic peak for rutile titania above 800 °C. Figure 5e shows the patterns of a 1:1 fiber/GMB sample, which contain the characteristic peak for anatase titania at every temperature and the characteristic peak for rutile titania above 650 °C. There was no cristobalite formation noted in these cases.

Catalyst-seeded samples

XRD patterns for the NiO-seeded samples are presented in Fig. 6. Figure 6a shows the XRD pattern



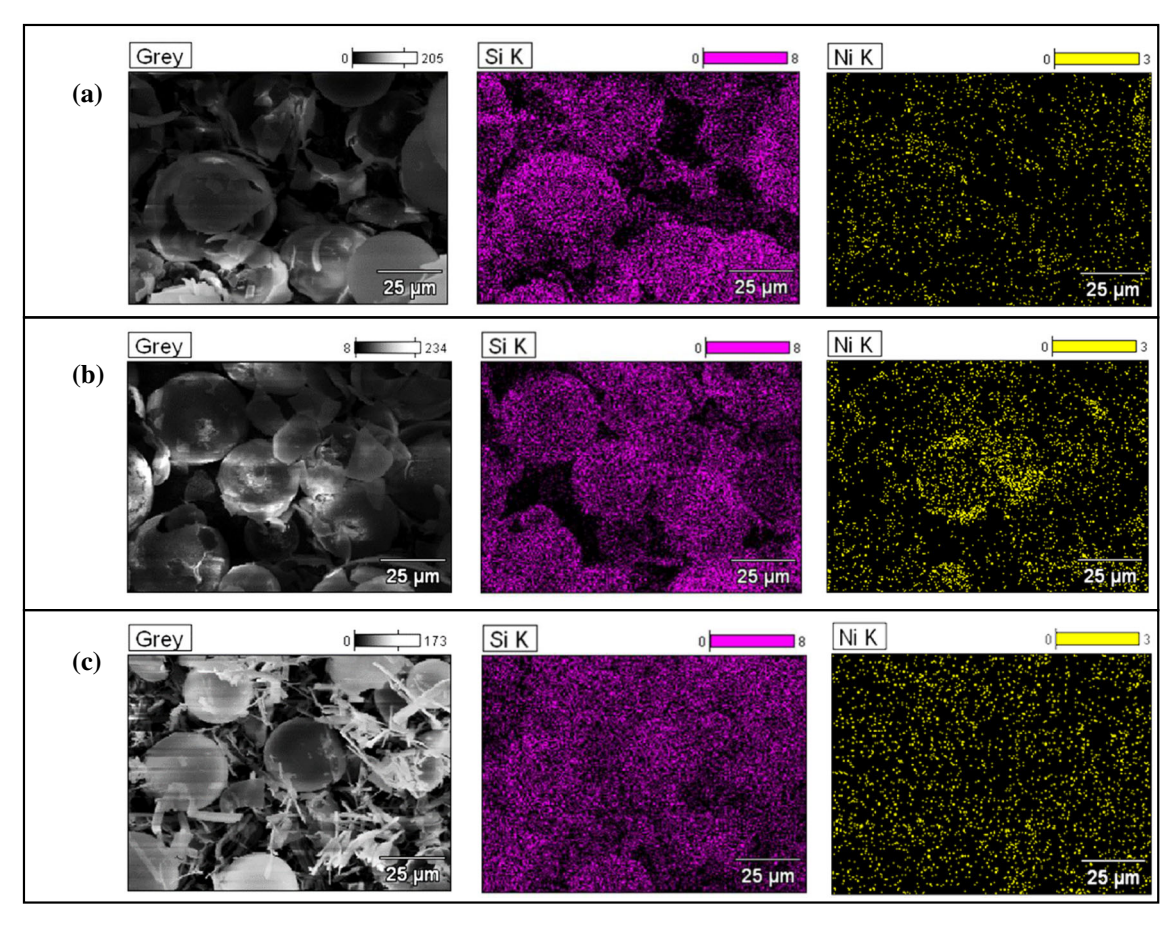


Figure 4 SEM images and EDS maps of **a** NiO-seeded GMBs, **b** NiO-seeded, titania-coated GMBs, and **c** a NiO-seeded SiO₂/GMB composite. The images on the left are BSE images followed by EDS maps of silicon in the middle and nickel on the right. The

EDS map for nickel for **a** has a noticeably sparser NiO coating than the other samples, which may be due to the smooth exterior of the uncoated GMBs.

before reaction, and Fig. 6b shows the XRD pattern after the catalytic reaction. Crystallite sizes were determined based on the data in Fig. 6, and they are given in Table 2. There was a small difference between the amounts of NiO on the surface of the different substrates before the reaction, with a larger amount of NiO observed on TiO2-coated GMBs. It was also determined that the GMBs crystallized to form cristobalite during the reaction, with smaller crystallites on average in the sample containing silica nanofibers. With respect to NiO, there is an increase in crystallite size that is to be expected with exposure to high temperatures. The formation of NiTiO₃ was detected in TiO₂-coated samples. It was also noted that the GMBs-SiO₂ sample showed less cristobalite formation due to higher temperature stability of silica fibers and better retention of NiO.

Atomic absorption spectrometry

AAS results of the NiO-seeded samples are given in Table 3. Despite both the titania-coated and composite samples having nearly the 5% Ni that was intended during processing, the uncoated GMBs had approximately half that. This may be due to the smooth surface of the GMBs when compared to the titania-coated GMBs, and the silica fibers may make up for that discrepancy in the composite material.

Mechanical testing

CS1 samples

Samples processed using CS1 binder solution did not express satisfactory mechanical properties. This can be the result of the TiO₂ layer delamination (Fig. 2). Indeed, both rectangular and cylindrical NF/GMB



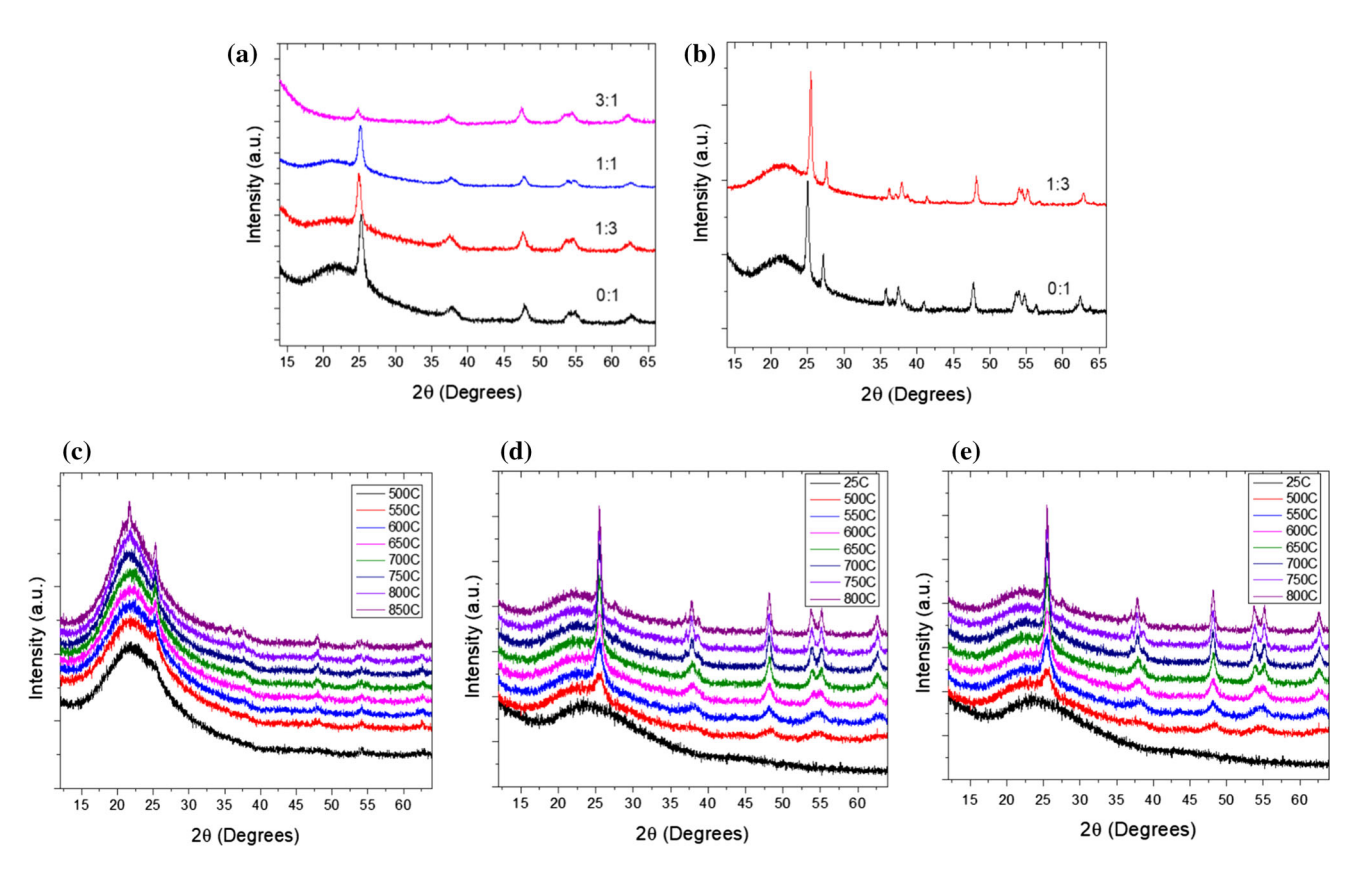


Figure 5 XRD patterns depicting the formation of anatase and rutile titania during the heat treatment of various silica nanofiber/GMB composite materials. Figures **a**, **b** depict patterns of samples prepared using CS1 and 500 °C and 700 °C, respectively. The

numbers above the patterns represent the mass ratio of fibers to GMB. Figures c–e are dynamic XRD results depicting the phase transformations in titania and silica from up to 850 $^{\circ}$ C in a samples with 0:1, 1:1, and 1:0 fiber/GMB ratios, respectively.

slabs were very weak mechanically after calcination at 500 °C and 700 °C. The GMB slabs were cracked, and NF/GMB slabs showed only 0.026 + 0.012 MPa maximum compression strength. No data were obtainable for a 0:1 fiber/GMB sample because the sample disintegrated upon handling. These results, along with the formation of NiTiO3 during the reaction, led to exclusion of such material from further testing.

CS2 samples

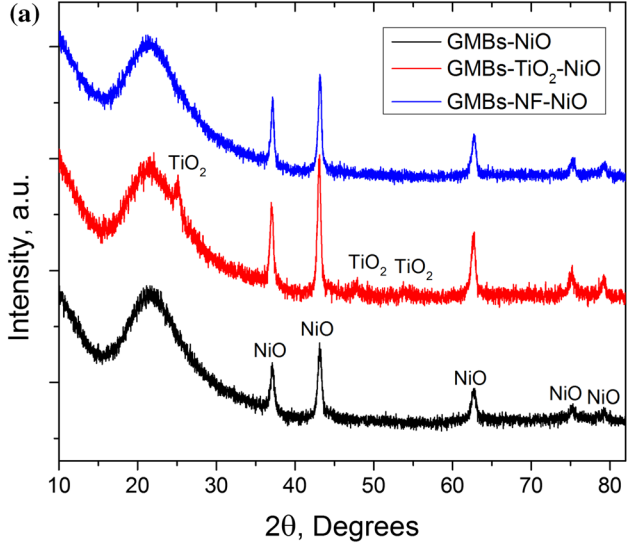
Samples processed using CS2 binder solution showed promise in their mechanical properties, and the data shown in Fig. 7 indicated a clear relationship between fiber content and strength of the composite in compression. As more fibers are added, the strength increases (Fig. 7c), which is expected due to the few contact points between round GMBs, while nanofibers resulted in more contact points between both fibers and GMBs. The density of the tested

materials increased from $0.14 \pm 0.03 \text{ g/cm}^3$ for GMBs to $0.19 \pm 0.02 \text{ g/cm}^3$ for 1:1 GMB/NF composite, and to $0.25 \pm 0.025 \text{ g/cm}^3$ for silica nanofiber (NF). Figure 7a and b shows stress/strain curves for the samples, and they indicate that, while the strength of the composite structures is lower than that of the fiber sample, the composite has a greater ductility. Also, the flexural strength was significantly lower than the compressive strength in all cases. This discrepancy can be associated with the anisotropy of stress distribution that depends on the loading direction, small thickness of the binder layer, and internal microarchitecture of tested materials [26].

Catalytic testing

Gas chromatography results from the methane-reforming reactions are summarized in Table 4. The conversion/selectivity numbers varied within 1% during the tests (except CH_4 conversion at 900 °C, and CO_2 selectivity which was always 100%). For the





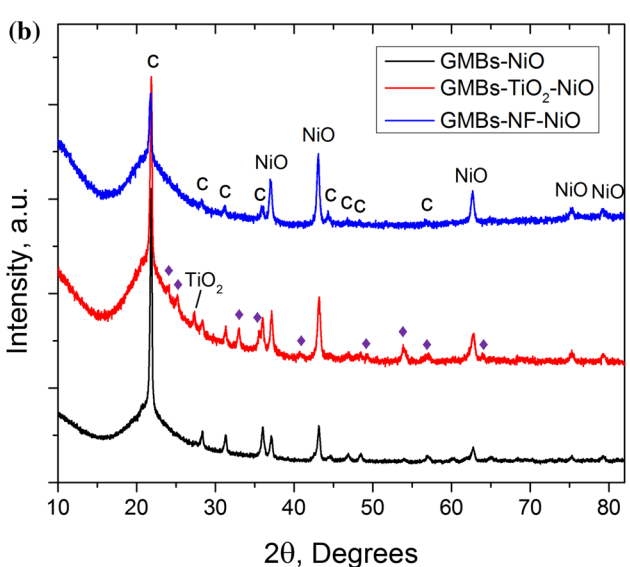


Figure 6 XRD patterns of NiO-seeded GMBs, TiO₂-GMBs, and GMBs-SiO₂ nanofibers samples before (**a**) and after (**b**) catalytic reaction. The patterns are normalized to the content of Ni determined from AAS data. Symbols (**c**) and (Filled diamond) indicate the cristobalite and NiTiO₃ phases, respectively.

uncoated GMBs and the TiO_2 -coated GMBs, there was only a negligible CH_4 conversion and no formation of the desired products regardless of temperature. The presence of TiO_2 also seems to harm the effectiveness of the NiO catalyst, which is particularly evident due to the increased amount of NiO on the surface of the GMBs shown in Fig. 6a and expected better performance. The most effective catalyst is the 1:1 fiber/GMB composite material, which has the highest CH_4 conversion at both temperatures and has a significant amount of both desired products at 900 °C. It is particularly significant that there is a 2:1 ratio of H_2 to CO in the products at 900 °C, indicating a successful reaction.

Discussion

The results from these preliminary trials suggest that the proposed approach can be suitable for the synthesis of a metal oxide-coated GMBs/SiO₂ composite syntactic foam that can be used either as a catalyst or as catalyst support. The SEM images show that the microballoons can be evenly coated with metal oxide (e.g., TiO₂), depending on the selected precursor, and that the coating is present on both the GMBs and the fibers. The broken GMBs in the images can be attributed to the treatment of the GMBs during processing or during sample preparation for SEM. In a slab structure, it is less likely that such breakage would occur. Delamination of the coating could be attributed to deformation of the GMBs when exposed to high temperatures, although the high-temperature deformation analysis conducted in this study indicates that there is likely another cause for coating delamination in those samples coated with CS1 binder solution. The samples produced using the

Table 2 Crystallite sizes for NiO and SiO₂ for catalytic samples before and after reactions

Sample	Before reaction		After reaction		
	NiO crystallite size (nm)	SiO ₂ crystallite size (nm)	NiO crystallite size (nm)	SiO ₂ crystallite size (nm)	
GMBs	15.3 ± 1.0	_	24.4 ± 0.1	27.0 ± 1.0	
TiO2-coated GMBs	17.6 ± 2.0	_	22.8 ± 2.0	25.3 ± 1.0	
Fiber/GMB composite	18.2 ± 1.0	-	22.8 ± 1.0	15.2 ± 1.0	

The data were calculated based on the XRD patterns found in Fig. 6 and show an increase in crystallite size for NiO for all samples and the formation of cristobalite



Table 3 AAS data showing the nickel content of each sample that was prepared for catalytic testing

Sample	Uncoated GMBs	TiO ₂ -coated GMBs	1:1 SiO ₂ fibers/GMBs
Ni content [mg/kg]	24112	47976	48808
Weight% Ni [w/w]	2.4	4.8	4.9

The uncoated GMBs did not retain much of the nickel during seeding and have less than half of the nickel content of the other two samples

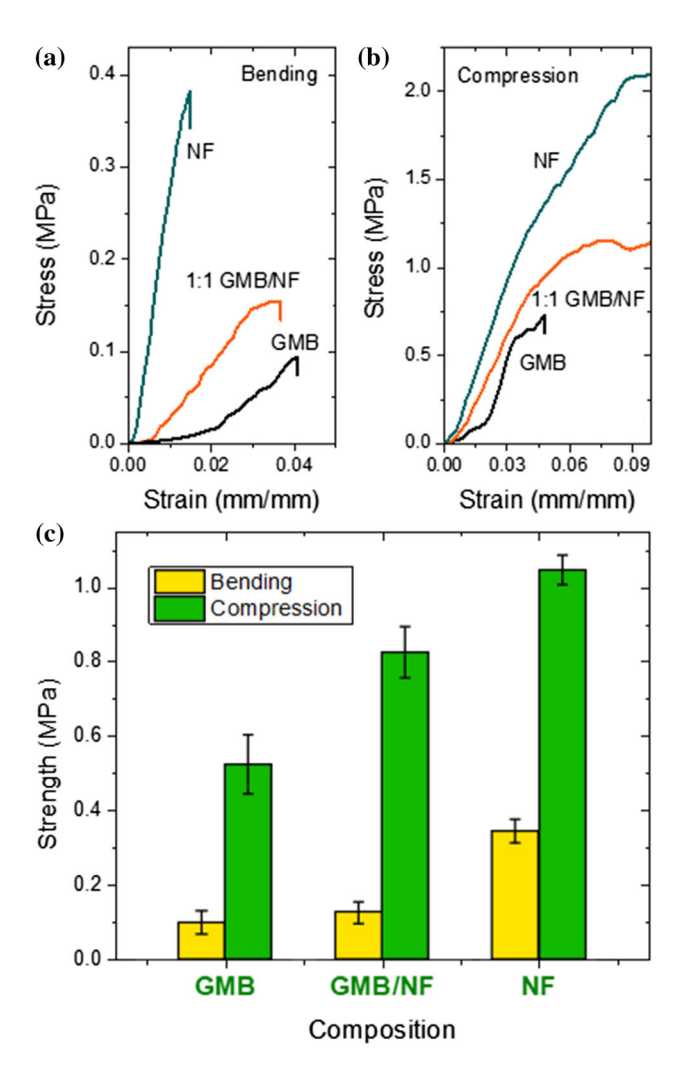


Figure 7 Mechanical data from samples coated using a TiOSO₄-based coating solution. Plots **a**, **b** are representative stress–strain curves for three samples varying in amounts of fibers and GMBs, and those compositions are listed adjacent to the curves. Plot **a** is the result of three-point bend tests, and **b** is the result of compression tests. Strength values are represented in plot (**c**). These plots indicate a high increase in strength with an increase in fiber content. Plots **a**, **b** also indicate higher ductility in samples with a lower fiber content. The samples also indicate much better performance in compression than in bending.

aqueous CS2 binder solution can be considered more successful, as they lack coating delamination at all temperatures tested in this study and have superior mechanical properties.

XRD patterns from the samples prepared using CS1 solution show preservation of a significant portion of nanocrystalline (crystallite size ~ 17 nm) anatase phase up to 700 °C. Such behavior is desired, as the anatase phase of titania is the most active phase for photocatalysis [27]. The samples coated using the CS2 solution tend to form rutile above 650 °C. XRD also revealed the formation of cristobalite in GMBs above 800 °C, which may contribute to the lack of thermally induced deformation in those samples treated at 800 °C or 1000 °C. The obtained data indicate the future need in development of the optimum precursor and procedure for metal oxide binder coating for achieving the desired function of syntactic foam.

The results of the flexural and compression tests of the composite materials indicate that further study into the behavior of this type of material is necessary. While a direct trend can be noted between fiber content and strength in those samples processed with CS2 binder solution, the data from CS1 samples were largely inconclusive. What can be determined based on the difference between CS1 and CS2 in terms of coating quality and mechanical strength is that the homogeneity and coverage of the coating/binder are highly important to the strength and handleability of the composite structure. While the mechanical strength of these materials is relatively low, it is clear that the addition of fibers to the syntactic foam greatly increased the compressive strength of the material. This is similar to the increase found in the literature with the addition of nanofibers to epoxyresin syntactic foams [4, 16–18], but this increase is most likely not a result of the same strengthening mechanisms found in those studies. In this material, there is less probability for crack bridging or crack blunting as the matrix is not a homogeneous bulk material, so the increase in mechanical strength with



Table 4 Methane conversion ratios and H_2 , CO, and CO_2 selectivity values determined through gas chromatography for three sample types at either 700 °C or 900 °C

Catalyst	Temperature (°C)	CH ₄ conversion (%)	H ₂ selectivity (%)	CO selectivity (%)	CO ₂ selectivity (%)
Uncoated GMBs $m = 0.103$ g	700 °C	1	0	0	100
	900 °C	12	0	0	100
$TiO_2 + GMBs m = 0.101 g$	700 °C	0	0	0	0
	900 °C	3	0	0	100
1:1 Fibers/GMBs $m = 0.104 \text{ g}$	700 °C	35	0	0	100
	900 °C	100	63	31	6

The most effective catalyst material was the 1:1 fibers/GMBs sample, which is notable due to its 100% conversion of methane and 2:1 ratio of H_2 to CO

the addition of fibers is most likely due to the increase in packing density and contact area between the components of the reinforcement. While this may not be evident with the increase in mechanical strength, those studies that added nanofibers to syntactic foams often saw an increase in the flexural modulus with an addition of a small amount of added nanofibers [4], but the fully ceramic system shows no improvement in flexural properties with the addition of 50% silica nanofibers. This departure from how fibers affect epoxy-resin syntactic foams indicates that other fracture mechanisms and other toughening mechanisms are at play, but there is still an improvement in compressive strength due to the addition of silica nanofibers.

The preliminary catalytic data suggest that GMB/fiber composite material can be suitable as a support of NiO catalyst for methane steam reforming. The surface of the GMBs by themselves may be too smooth to provide support for catalyst particles and sufficient number of active sites for catalysis. In the case of the titania-coated sample, there is evidence to suggest that titania may weaken the catalytic properties of transition metal catalysts in methane reforming [28], but other work suggests that titania may be a suitable catalysts if the reaction temperature is kept low (~ 500 °C) to prevent the formation of NiTiO₃ [29]. Methane steam reforming is typically carried out above 800 °C in industry, but further work with titania and other metal oxides must be done to determine its efficacy when used on GMBs or in fiber/GMB composites. The high activity of the fiber/GMB composite material may be due to the higher resident time of reactants at the catalyst surface or due to the more favorable energy state of the nanofiber surface. The activities found for the composite material are comparable to other silica-supported nickel-based catalysts in steam-reforming processes [10], and the conversion is also comparable to nickel nanoparticles with no support material [30]. These preliminary data suggest that a composite structure silica fibers and GMBs may function as a suitable support material for steam methane reformation and similar processes.

Conclusions

The results of this experiment show a proof of concept that a syntactic foam constructed out of GMBs, silica nanofibers, and a titania or other metal oxide coating may be applicable as a catalyst or catalyst support. The use of titania as a binder provides suitable binding of the base materials, and the addition of nanofibers to the pure-GMB syntactic foam greatly increased the handleability and strength of the resultant material. The preservation of the anatase phase further supports the possible use of this material as a photocatalyst. The composite structure of silica nanofibers with GMBs shows promise for use as catalyst support for transition metal catalysts, but the use of a titania or other oxide binder should be considered in each specific application. Further studies need to be done on the mechanical and catalytic properties of such composite materials, depending on the precursors for metal oxide binder and the fabrication procedure.



Acknowledgements

This work has been supported in part by the National Science Foundation (NSF) [Grant Number DMR-1708600]. MA, SN, and CS thank the support from the NSF International Research Experience for Students (IRES) Program [Grant Number OISE-1558268].

Compliance with ethical standards

Conflict of interest There are no relationships or interests of the authors of this work that may bias the results of this work.

References

- Brown JA, Carroll JD, Huddleston B, Casias Z, Long KN (2018) A multiscale study of damage in elastomeric syntactic foams. J Mater Sci 53(14):10479–10498
- [2] Jayavardhan ML, Doddamani M (2018) Quasi-static compressive response of compression molded glass microballoon/HDPE syntactic foam. Compos B Eng 149:165–177
- [3] Panteghini A, Bardella L (2015) On the compressive strength of glass microballoons-based syntactic foams. Mech Mater 82:63–77
- [4] Dimchev M, Caeti R, Gupta N (2010) Effect of carbon nanofibers on tensile and compressive characteristics of hollow particle filled composites. Mater Des 31(3):1332–1337
- [5] Koopman M, Chawla K, Ricci W, Carlisle K, Gladsyz G, Lalor M, Jones M, Kerr K et al (2009) Titania-coated glass microballoons and cenospheres for environmental applications. J Mater Sci 44(6):1435–1441
- [6] Yao H, Xie Y, Jing Y, Wang Y, Luo G (2017) Controllable preparation and catalytic performance of heterogeneous fenton-like α-Fe2O3/crystalline glass microsphere catalysts. Ind Eng Chem Res 56(46):13751–13759
- [7] An Y, Zheng P, Ma X (2019) Preparation and visible-light photocatalytic properties of the floating hollow glass microspheres—TiO2/Ag3PO4 composites. RSC Adv 9(2):721–729
- [8] Cheng B, Chen X, Wang X, Qiu H, Qi S (2017) Preparation and microwave absorbing performance of TiO2/ NiFe2O4 / hollow glass microsphere composite with core–shell structure. J Mater Sci Mater Electron 28(11):7575–7581
- [9] Guo X, Sun Y, Yu Y, Zhu X, Liu C-J (2012) Carbon formation and steam reforming of methane on silica supported nickel catalysts. Catal Commun 19:61–65
- [10] Amin MH (2020) Relationship between the pore structure of mesoporous silica supports and the activity of nickel

- nanocatalysts in the CO2 reforming of methane. Catalysts (2073–4344) 10(1):51
- [11] Ye R-P, Gong W, Sun Z, Sheng Q, Shi X, Wang T, Yao Y, Razink JJ et al (2019) Enhanced stability of Ni/SiO2 catalyst for CO2 methanation: Derived from nickel phyllosilicate with strong metal-support interactions. Energy 188:116059
- [12] Tao M, Meng X, Lv Y, Bian Z, Xin Z (2016) Effect of impregnation solvent on Ni dispersion and catalytic properties of Ni/SBA-15 for CO methanation reaction. Fuel 165:289–297
- [13] Matsumura Y, Nakamori T (2004) Steam reforming of methane over nickel catalysts at low reaction temperature. Appl Catal A 258(1):107–114
- [14] Rodemerck U, Schneider M, Linke D (2017) Improved stability of Ni/SiO2 catalysts in CO2 and steam reforming of methane by preparation via a polymer-assisted route. Catal Commun 102:98–102
- [15] John B, Reghunadhan Nair CP (2014) 13-Syntactic foams, in handbook of thermoset plastics (Third Edition), In: Dodiuk H, Goodman SH (Eds.) William Andrew Publishing: Boston. pp 511–554
- [16] Zhang L, Ma J (2013) Effect of carbon nanofiber reinforcement on mechanical properties of syntactic foam. Mater Sci Eng A 574:191–196
- [17] Colloca M, Gupta N, Porfiri M (2013) Tensile properties of carbon nanofiber reinforced multiscale syntactic foams. Compos B Eng 44(1):584–591
- [18] Ullas AV, Qayyum B, Kumar D, Roy PK (2016) Electrospun polyamide nanofiber-reinforced hybrid syntactic foams. Polym Plastics Technol Eng 55(17):1797–1806
- [19] He S, Carolan D, Fergusson A, Taylor AC (2019) Toughening epoxy syntactic foams with milled carbon fibres: mechanical properties and toughening mechanisms. Mater Des 169:107654
- [20] Karthikeyan CS, Sankaran S, Kishore (2000) Influence of chopped strand fibres on the flexural behaviour of a syntactic foam core system. Polym Int 49(2):158–162
- [21] Karthikeyan CS, Sankaran S, Jagdish Kumar MN, Kishore (2001) Processing and compressive strengths of syntactic foams with and without fibrous reinforcements. J Appl Polym Sci 81(2):405–411
- [22] Karthikeyan CS, Sankaran S, Kishore (2004) Elastic behaviour of plain and fibre-reinforced syntactic foams under compression. Mater Lett 58(6):995–999
- [23] Karthikeyan CS, Sankaran S, Kishore (2005) Flexural behaviour of fibre-reinforced syntactic foams. Macromol Mater Eng 290(1):60–65
- [24] Stanishevsky A, Tchernov J (2019) Mechanical and transport properties of fibrous amorphous silica meshes and



- membranes fabricated from compressed electrospun precursor fibers. J Non Cryst Solids 525:119653
- [25] Wang H, Jiao C, Zhao L, Chen X (2018) Preparation and characterization of TiO2-coated hollow glass microsphere and its flame-retardant property in thermoplastic polyurethane. J Therm Anal Calorim 131(3):2729–2740
- [26] Alaoui AH, Woignier T, Scherer GW, Phalippou J (2008) Comparison between flexural and uniaxial compression tests to measure the elastic modulus of silica aerogel. J Non Cryst Solids 354(40):4556–4561
- [27] Herrmann J-M (1999) Heterogeneous photocatalysis: fundamentals and applications to the removal of various types of aqueous pollutants. Catal Today 53(1):115–129

- [28] Mohamedali M, Amr H, Ibrahim H (2018) Recent advances in supported metal catalysts for syngas production from methane. ChemEngineering 2(1):9
- [29] Kho ET, Scott J, Amal R (2016) Ni/TiO2 for low temperature steam reforming of methane. Chem Eng Sci 140:161–170
- [30] Ali S, Al-Marri MJ, Abdelmoneim AG, Kumar A, Khader MM (2016) Catalytic evaluation of nickel nanoparticles in methane steam reforming. Int J Hydrogen Energy 41(48):22876–22885

Publisher's Note Springer Nature remains neutral with regard to jurisdictional claims in published maps and institutional affiliations.

